Proceedings of the Korean Nuclear Society Spring Meeting
Kwangju, Korea, May 2002

Analytic Function Expansion Nodal Method in R-Z Coordinates for Analysis of PBMR Cores

Do Sam Kim and Nam Zin Cho

Korea Advanced Institute of Science and Technology
373-1 Kusong-dong, Yusong-gu
Taejon, Korea 305-701

Abstract

In this paper, we extend the analytic function expansion nodal (AFEN) method to the cylindrical nodes by introducing analytic basis functions in R-Z coordinates and report the results of two benchmark problems, one of which is a PBMR core containing a truncated cone.

I. Introduction

There is growing interest in developing pebble bed modular reactors (PBMRs)[1]. The core of a PBMR typically contains a portion of truncated cone shape in cylindrical geometry. This paper reports for the first time development of a modern nodal solver for PBMR cores. We extend the current AFEN method[2,3] to treat the cylindrical node which arises in the analysis of pebble bed modular reactors. The Laplacian term in the diffusion equation has a different form in R-Z coordinates compared with that in Cartesian coordinates. Thus, we formulate an AFEN method in R-Z coordinates which includes the use of Bessel functions or modified Bessel functions. In addition to the rectangular nodes, we also consider triangular nodes. The numerical results obtained to test the accuracy indicate the method's applicability to practical problems.

II. Methodology

II.1 Basis functions

The AFEN formulation in the R-Z coordinates system starts from the following two-group diffusion equations in a node:

$$-\nabla^2 \vec{\phi}(z,r) - [A]\vec{\phi}(z,r) = 0, \tag{1}$$

where

$$[A] = [D]^{-1}\left([\Sigma] - \frac{[\nu\Sigma_f]}{k_{eff}}\right).$$

All the notations are standard. For simplicity, we omitted the node index in this section. In the AFEN method, the equation is decomposed by introducing a new variable ξ defined by

$$\vec{\phi} = [R]\,\vec{\xi}, \quad [R] = [e_1, e_2], \tag{2}$$

where e_μ (μ=1,2) is an eigenvector of $[A]$ with the corresponding eigenvalues λ_μ. After the transformation, Eq.(1) is decoupled as

$$\nabla^2 \xi_\mu(z,r) - \lambda_\mu \xi_\mu(z,r) = 0, \quad \mu = 1,2. \tag{3}$$

This equation can be rewritten in the R-Z coordinates as follows:

$$\frac{\partial^2 \xi_\mu}{\partial r^2} + \frac{1}{r}\frac{\partial \xi_\mu}{\partial r} + \frac{\partial^2 \xi_\mu}{\partial z^2} - \lambda_\mu \xi_\mu = 0\,. \tag{4}$$

The analytic basis functions of the radial part in this equation are Bessel functions or modified Bessel functions depending on the sign of λ_μ's. The analytic basis functions of the axial part are identical to those of the Cartesian coordinates system. Thus, we can expand $\xi_\mu(z,r)$ by using these analytic basis functions as follows:

$$\xi_\mu(z,r)=\begin{cases} a_{\mu,0}+a_{1\mu,}I_0(k_\mu r)+a_{\mu,2}K_0(k_\mu r) \\ +a_{\mu,3}\sinh(k_\mu z)+a_{\mu,4}\cosh(k_\mu z) \\ +a_{\mu,5}I_0(\frac{k_\mu r}{\sqrt{2}})\sinh(\frac{k_\mu z}{\sqrt{2}})+a_{\mu,6}I_0(\frac{k_\mu r}{\sqrt{2}})\cosh(\frac{k_\mu z}{\sqrt{2}}) \\ +a_{\mu,7}K_0(\frac{k_\mu r}{\sqrt{2}})\sinh(\frac{k_\mu z}{\sqrt{2}})+a_{\mu,8}K_0(\frac{k_\mu r}{\sqrt{2}})\cosh(\frac{k_\mu z}{\sqrt{2}}), \quad (\lambda_\mu>0), \\ \\ a_{\mu,0}+a_{\mu,1}J_0(k_\mu r)+a_{\mu,2}Y_0(k_\mu r) \\ +a_{\mu,3}\sin(k_\mu z)+a_{\mu,4}\cos(k_\mu z) \\ +a_{\mu,5}J_0(\frac{k_\mu r}{\sqrt{2}})\sin(\frac{k_\mu z}{\sqrt{2}})+a_{\mu,6}J_0(\frac{k_\mu r}{\sqrt{2}})\cos(\frac{k_\mu z}{\sqrt{2}}) \\ +a_{\mu,7}Y_0(\frac{k_\mu r}{\sqrt{2}})\sin(\frac{k_\mu z}{\sqrt{2}})+a_{\mu,8}Y_0(\frac{k_\mu r}{\sqrt{2}})\cos(\frac{k_\mu z}{\sqrt{2}}), \qquad (\lambda_\mu<0), \end{cases} \tag{5}$$

where

I_0 : the first kind modified Bessel function of order 0,

K_0 : the second kind modified Bessel function of order 0,

J_0 : the first kind Bessel function of order 0,

Y_0 : the second kind Bessel function of order 0,

$k_\mu=\sqrt{|\lambda_\mu|}$.

The coefficients in Eq.(5) can be expressed in terms of nodal unknowns shown in Fig.1. In the figure, *k* is axial node index and *i* is radial node index. $\vec{\phi}_{k,i}^{av}$ is node average flux, $\vec{\phi}_{k,i}^{st}(s=z,r;t=0,1)$ are four interface average fluxes and $\vec{\phi}_{k,i}^{uv}(u=0,1;v=0,1)$ are four edge fluxes.

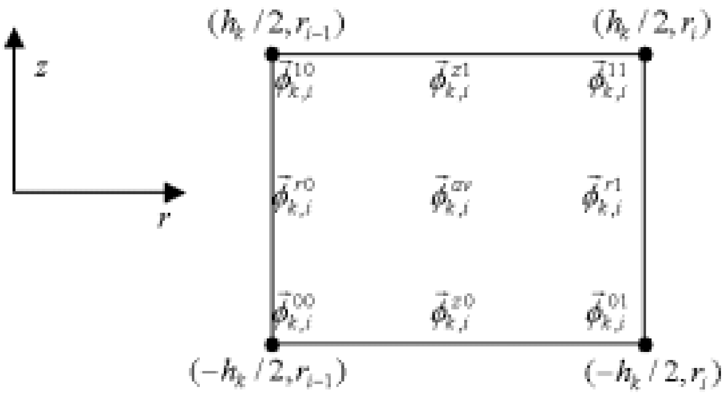

Fig.1. Nodal unknowns in rectangular node (k,i)

II.2 Nodal coupling equations

By using Eqs.(2) and (5), we write the interface average currents in *r* and *z* direction as follows:

$$\vec{J}_{k,i}^{z0} = \vec{J}_{k,i}^{z}\left(-\frac{h_z}{2}\right), \vec{J}_{k,i}^{z1} = \vec{J}_{k,i}^{z}\left(\frac{h_z}{2}\right), \vec{J}_{k,i}^{r0} = \vec{J}_{k,i}^{r0}(r_{i-1}), \vec{J}_{k,i}^{r1} = \vec{J}_{k,i}^{r}(r_i), \tag{6}$$

where

$$\vec{J}_{k,i}^{z}(z) = -[D][R]\frac{\int_{r_{i-1}}^{r_i} r\frac{d}{dz}\vec{\phi}(z,r)dr}{\int_{r_{i-1}}^{r_i} r\,dr},$$

$$\vec{J}_{k,i}^{r}(r) = -[D][R]\frac{\int_{-h_k/2}^{h_k/2}\frac{d}{dr}\vec{\phi}(z,r)dz}{h_k}.$$

After some manipulations, all the currents at the interfaces are expressed in terms of nodal unknowns. For example,

$$\begin{aligned}\vec{J}_{k,i}^{z0} = {} & [M_{k,i}^{av}]\vec{\phi}_{k,i}^{av} + [M_{k,i}^{z0}]\vec{\phi}_{k,i}^{z0} + [M_{k,i}^{z1}]\vec{\phi}_{k,i}^{z1} + [M_{k,i}^{r0}]\vec{\phi}_{k,i}^{r0} + [M_{k,i}^{r1}]\vec{\phi}_{k,i}^{r1} \\ & + [M_{k,i}^{00}]\vec{\phi}_{k,i}^{00} + [M_{k,i}^{01}]\vec{\phi}_{k,i}^{01} + [M_{k,i}^{r0}]\vec{\phi}_{k,i}^{10} + [M_{k,i}^{r1}]\vec{\phi}_{k,i}^{11},\end{aligned} \tag{7}$$

where M's are 2x2 coefficient matrices. The first nodal coupling equation is node balance equation which is obtained from the integration of the diffusion equation over a node,

$$\frac{\vec{J}_{k,i}^{z1} - \vec{J}_{k,i}^{z1}}{h_k} + \frac{2\left(r_i\vec{J}_{k,i}^{r1} - r_{i-1}\vec{J}_{k,i}^{r0}\right)}{r_i^2 - r_{i-1}^2} + [\Sigma]\phi_{k,i}^{av} = \frac{[\nu\Sigma_f]}{k_{eff}}\phi_{k,i}^{av}. \tag{8}$$

By replacing the currents written in the form of Eq.(7), we obtain an equation for the node average fluxes. The second nodal coupling equations for the interface average fluxes are obtained by applying the continuity conditions of the currents across the interface. The third nodal coupling equations are required to update the edge fluxes. These equations are derived on the basis of the source-free condition around an edge. By applying this condition, edge flux $\vec{\phi}_{k,i}^{11}$ shared by four nodes is found in the following form:

$$\left(\sum_j [T_j]\right)\vec{\phi}_{k,i}^{11} = \sum_j\left([T_j^{av}]\vec{\phi}_j^{av} + \sum_{d=r,z}\sum_{s=0,1}[M_{k,i}^{ds}]\vec{\phi}_{k,i}^{ds} + \sum_{d=0,1}\sum_{s=0,1}[M_{k,i}^{ds}]\vec{\phi}_{k,i}^{ds}\right), \tag{9}$$

where

$$j = (k,i), (k+1,i), (k,i+1) \text{ and } (k+1,i+1),$$
$$[T]\text{'s} : \text{2x2 coefficient matrices.}$$

As in the conventional nodal methods, the iteration procedure in the AFEN method requires two-level iterations (inner and outer) to solve the reactor eigenvalue problem. The inner iteration consists of three kinds of sweeps: edge flux sweep, interface flux sweep and volume-average flux sweep.

II.2 Treatment of triangular node for the pebble bed modular reactor (PBMR)

In the analysis of a pebble bed modular reactor, there are some regions which should be modeled in triangular nodes. Such a triangular node appears in the lower boundary of the pebble bed reactor. To simplify the formulation, we allocate an equal number of nodal unknowns to that of a rectangular node, which is shown in Fig. 2. In this case, $\phi_{k,i}^{z1}$ and $\phi_{k,i}^{z1}$ are the two half-line averaged fluxes along an oblique side. $\phi_{k,i}^{11}$ denotes the fulx at the mid-point of the oblique side. Except this, all the procedures of the formulation are similar to those of the rectangular nodes.

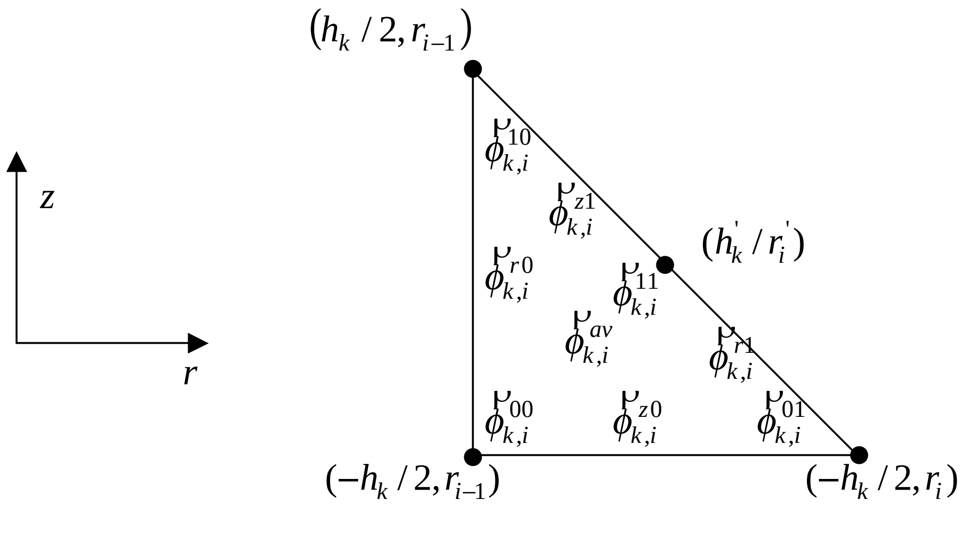

Fig.2. Nodal unknowns in triangular node (k,i)

III. Numerical Results

To show the performance of the newly developed code, two benchmark problems were solved. Benchmark Problem I was obtained from the initial core of the two-dimensional (R-Z) reactor model given in the Ref. 4. Benchmark Problem II was obtained by modifying the lower part of Benchmark Problem I reactor to have triangular nodes by removing the reflector region. The core contains a portion of truncated cone shape, that typically represents a PBMR core. The reactor configurations are shown in Fig. 3 and the cross sections of the regions are given in Table 1.

Table 2 shows the results of Benchmark Problem I. It shows that even for Case 1 where the biggest node size is 150 cm $\times$80 cm, the AFEN method gives accurate results in predicting the multiplication factor and the regional average powers. Due to the limitation of the computer memory, the results of the VENTURE code are compared only with those of Case 3 in AFEN. To compare the relative accuracy between the AFEN method and an existing nodal method, Table 3 shows the results of a semi-analytic nodal code reported in Ref. 5. The results indicate that the radial node size should be less than 10cm at least to obtain an acceptable accuracy in the multiplication factor when using a semi-analytic nodal method.

Table 4 shows the results of Benchmark Problem II. The AFEN results of the two cases of varying node size are very accurate both in the multiplication factor and in the regional average powers. The difference in the regional power becomes larger in the lower part of the core. However, the maximum regional power difference in Region 12 between Cases 1 and 2 is only 0.64%.

IV. Conclusions

We developed a modern nodal solution method of AFEN formulation in R-Z geometry for analysis of PBMR cores. In addition to the rectangular nodes, we also included triangular nodes which can be used to model the truncated cone shape of a PBMR core. The results of two benchmark problems show that the AFEN method gives solutions of very high accuracy.

References

1. A. C. Kadak, D. A. Petti, et al., Idaho National Engineering & Environmental Laboratory. *Modular Pebble Bed Reactor Project University Research Consortium Annual Report*, INEEL/EXT-2000-01034, July 2000.
2. J. M. Noh and N. Z. Cho, "A New Approach of Analytic Basis Function Expansion to Neutron Diffusion Nodal Calculation," *Nucl. Sci. Eng.*, **116**, 165 (1994).
3. N. Z. Cho and J. M. Noh, "Analytic Function Expansion Nodal Method for Hexagonal Geometry," *Nucl. Sci. Eng.*, **121**, 245 (1995).
4. Argonne National Laboratory. *Argonne Code Center: Benchmark Problem Book,* ANL-7416, Supplement 2 (1977).
5. 김종경, "R-Z좌표계에 대한 중성자 확산방정식의 해석적 노달전개법 개발 연구," 제 4차 신형원자로 연구센터 연구발표회 논문집 – 신형원자로의 노심핵 특성 연구,제 6장, CARR/RCA-9601, 1996.+6

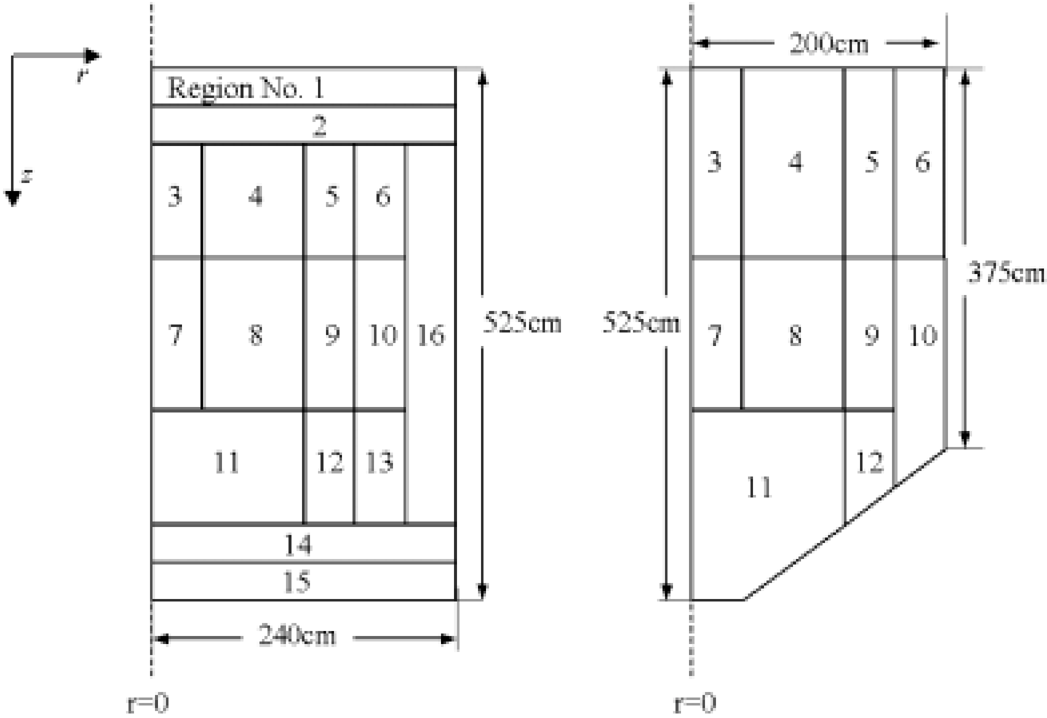

(a) Benchmark Problem I (b) Benchmark Problem II

Fig. 3. Core configurations of the benchmark problems (R-Z view)

Table 1. Macroscopic cross sections of the benchmark problems

Region	Group	$D_g(cm)$	$\Sigma_a(cm^{-1})$	$\Sigma_{1\to 2}(cm^{-1})$	$\nu\Sigma_f(cm^{-1})$
1,15	1	1.0684E+00	2.0000E-03	2.6000E-02	0.0000E+00
	2	3.2051E-01	3.3000E-03	0.0000E+00	0.0000E+00
2,14	1	1.3495E+00	1.0000E-05	1.2000E-02	0.0000E+00
	2	8.7032E-01	1.9000E-02	0.0000E+00	0.0000E+00
3,4,11	1	1.3052E+00	2.4399E-03	8.0351E-03	1.1776E-03
	2	8.8857E-01	1.3063E-02	0.0000E+00	1.3268E-02
5,12	1	1.3052E+00	2.4399E-03	8.0351E-03	1.1776E-03
	2	8.8857E-01	1.2623E-02	0.0000E+00	1.3268E-02
6,13	1	1.3052E+00	2.4399E-03	8.0351E-03	1.1776E-03
	2	8.8857E-01	1.2183E-02	0.0000E+00	1.3268E-02
7,8	1	1.3052E+00	2.4399E-03	8.0351E-03	1.1776E-03
	2	8.8857E-01	1.3453E-02	0.0000E+00	1.3268E-02
9	1	1.3052E+00	2.4399E-03	8.0351E-03	1.1776E-03
	2	8.8857E-01	1.2973E-02	0.0000E+00	1.3268E-02
10	1	1.3052E+00	2.4399E-03	8.0351E-03	1.1776E-03
	2	8.8857E-01	1.2933E-02	0.0000E+00	1.3268E-02
16	1	1.2997E+00	2.5639E-03	7.9061E-03	1.2875E-03
	2	8.7951E-01	1.3065E-02	0.0000E+00	1.4246E-02

Table 2. Results of Benchmark Problem I

Code	AFEN			VENTURE
	Case 1	Case 2	Case 3	
Node Size $\Delta r(cm) \times \Delta z(cm)$	Irregular [a]	40×37.5	20×18.75	
$N_z{}^b \times N_r{}^c$	7×5	14×10	28×20	896×384 [d]
k_{eff} (%error [e])	0.8671966 (0.00147)	0.8671834 (-5.41E-5)	0.8671838	0.8671856 (0.00020)
Region	Normalized power (%error [e])			
3	1.2038 (-0.13)	1.2062 (0.07)	1.2053	1.2046 (-0.06)
4	1.2056 (-0.20)	1.2082 (0.01)	1.2081	1.2065 (-0.13)
5	1.1746 (-0.28)	0.1770 (-0.08)	1.1779	1.1755 (-0.20)
6	0.8972 (-0.39)	0.8993 (-0.15)	0.9007	0.8986 (-0.23)
7	1.7630 (0.10)	1.7639 (0.16)	1.7612	1.7639 (0.15)
8	1.7516 (0.06)	1.7522 (0.09)	1.7506	1.7521 (0.08)
9	1.6658 (0.03)	1.6658 (0.03)	1.6654	1.6656 (0.01)
10	1.2228 (0.13)	1.2214 (0.02)	1.2212	1.2208 (-0.03)
11	1.2069 (0.25)	1.2048 (0.08)	1.2038	1.2063 (0.21)
12	1.1762 (0.18)	1.1739 (-0.01)	1.1740	1.1755 (0.13)
13	0.8984 (0.07)	0.8970 (-0.09)	0.8977	0.8986 (0.10)
16	0.3932 (-0.06)	0.3932 (-0.07)	0.3935	0.3932 (-0.07)

[a] 40, 80, 40 and 40 in the radial direction
37.5, 37.5, 112.5, 150, 112.5, 37.5 and 37.5 in the axial direction

[b] number of axial nodes

[c] number of radial nodes

[d] Because the node size of 0.58cm×0.625cm in the FDM calculation is not small enough to compare the accuracy of 0.2% in the regional average power, the results of AFEN Case 3 are used as the reference.

[e] The reference is the results of AFEN Case 3

Table 3. Multiplication factors obtained from the CYLANEM code[5]
for Benchmark Problem I

Mesh Size	Δr (cm)	Irregular [a]	20	20	10	10
	Δz(cm)		37.5	18.75	37.5	18.75
k_{eff}		0.8633767	0.8663588	0.8663212	0.8669894	0.8670472
(%error [b])		(-0.424)	(-0.080)	(-0.084)	(-0.007)	(-0.00068)
(%error [c])		(-0.439)	(-0.095)	(-0.099)	(-0.022)	(-0.015)

[a] 40, 80, 40 and 40 in the radial direction

37.5, 37.5, 112.5, 150, 112.5, 37.5 and 37.5 in the axial direction

[b] Reference k_{eff} is 0.867053, which was reported in Ref. 4 (FDM calculation with node size 8cm×18.75cm).

[c] The reference is the results of AFEN Case 3

Table 4. Results of Benchmark Problem II

	Case 1	Case 2
Node Size $\Delta r(cm) \times \Delta z(cm)$	40×37.5	20×18.75
$N_r{}^{b} \times N_z{}^{c}$	14×10	28×20
k_{eff}	0.8573390 (-7.0E-4 [d])	0.8573450
Region	Normalized power	
3	2.3164 (0.11 [d])	2.3138
4	1.9218 (0.12)	1.9195
5	1.2839 (0.13)	1.2823
6	0.4628 (0.12)	0.4623
7	2.0647 (-0.01)	2.0649
8	1.6910 (-0.02)	1.6915
9	1.0992 (-0.06)	1.0999
10	0.3150 (-0.25)	0.3157
11	0.6054 (-0.32)	0.6073
12	0.3944 (-0.64)	0.3970

[a] 40, 80, 40 and 40 in the radial direction
37.5, 37.5, 112.5, 150, 112.5, 37.5 and 37.5 in the axial direction

[b] number of radial nodes

[c] number of axial nodes

[d] % difference of Case 1 from Case 2